



Research paper

Single-stranded DNA adsorption characteristics by hollow spherule allophane nano-particles: pH dependence and computer simulation



Yoko Matsuura, Shuichi Arakawa, Masami Okamoto*

Advanced Polymeric Nanostructured Materials Engineering, Graduate School of Engineering, Toyota Technological Institute, 2-12-1 Hisakata, Tempaku, Nagoya 468 8511, Japan

ARTICLE INFO

Article history:

Received 21 May 2014

Received in revised form 16 September 2014

Accepted 17 September 2014

Available online 7 October 2014

Keywords:

Natural allophane

Single-stranded DNA

Adsorption

MO simulation

ABSTRACT

Clay mineral surfaces have been important for the prebiotic organization and protection of nucleic acids. The morphological observation to provide insight into the adsorption structure and characteristics of single-stranded DNA (ss-DNA) by natural allophane particles was presented. The molecular orbital (MO) computer simulation has been used to probe the interaction of ss-DNA and/or adenosine 5'-monophosphate and allophane with active sites. Our simulations predicted that the strand undergoes some extent of the elongation, which induces the alteration of the conformation of the phosphate backbone, base–base distance and excluded volume correlation among bases. This work demonstrates the ss-DNA adsorption by the allophane particles with novel insights into the morphological features and detailed molecular level information. The overall results support a general adsorption mechanism for the ss-DNA/allophane complexation.

© 2014 Elsevier B.V. All rights reserved.

1. Introduction

Clay minerals, comprising a family of layer silicate, are the most ubiquitous nanoscale materials in soil. Smectites (e.g., montmorillonite (Mt), hectorite and saponite) are for the most part inherited from the parent rock, i.e., weathering processes (Wilson, 1999). Clay minerals have also been proposed as a vital role in the origins of life. One of the leading theories regarding the origins of life is the RNA world hypothesis (Gilbert, 1986), in which ribozyme plays important roles both as information molecules and enzymes and has been made at the very beginning of the origins of life (Dworkin et al., 2003). However, the RNA world hypothesis would have required a special environment, in the least as protection of extracellular RNA and deoxyribonucleic acid (DNA) molecules from hydrolysis and ultraviolet. Besides such environments have generated particular interest as a possible source of the first life forms (Wächtershäuser, 2006).

The ultraviolet degrades extracellular RNA and DNA molecules produced through this hypothesis. For the protection of DNA, the adsorption of DNA molecules on clay particles may be significant, as it shall give insights into the origin of life and subsequent survival of the same on this planet. Moreover, the persistent ability of the DNA molecules could transform competent cells when the DNA molecules bound to clay minerals and humic acids (Stotzky, 2000).

In addition, the confinement of cell membranes may have also played an important role for prebiotic compartmentalization in early life evolution. Many different environments have been considered for

this pre-cellular evolutionary stage (Ferris et al., 1996; Joyce, 2002; Trevors and Pollack, 2005).

In this regard, allophane is a short-range-order clay mineral and occurs in some soils derived from volcanic ejecta and is able to protect the extracellular DNA and RNA molecules from ultraviolet light. The primary particle of the allophane is a hollow spherule with an outer diameter of 3.5–5.0 nm and a wall of about 0.6–1.0 nm thick (as shown in Fig. S1a, b) (Brigatti et al., 2006; Iyoda et al., 2012). In addition to this large surface area, the (OH)Al(OH₂) groups exposed on the wall perforations are the source of the pH-dependent charge characteristics of allophane.

It is possible to investigate the origin of the living organisms and environments of the ancient earth by researching DNA in allophane clusters of the soil. The adsorption behavior of DNA or RNA molecules on allophane particles has been investigated. Many researchers have discussed the adsorption by using the Langmuir adsorption equation without deep insights into the morphological feature (Cleaves et al., 2011; Saeki et al., 2010; Taylor and Wilson, 1979).

In previous study (Matsuura et al., 2013), the morphology observation to provide insight into the adsorption structure and characteristics of single-stranded DNA (ss-DNA) by the allophane particles was examined, which was the first time of the real images obtained from microscopic experiment.

After the adsorption of DNA molecules on the allophane surface, the hydrogel was formed in the clustered allophane particles (Kawachi et al., 2013). The hydrogels based on DNA molecules and natural allophane clusters should also be useful in the conception of new forms of drugs release with highly-specific dosage and an improvement of the technological and biopharmaceutical properties in clay polymer nanocomposite hydrogels (Kevadiya et al., 2010, 2012; Silva et al., 2009; Yuan et al., 2010). The adsorption of DNA to mineral surfaces is of

* Corresponding author. Tel.: +81 528091861; fax: +81 528091864.
E-mail address: okamoto@toyota-ti.ac.jp (M. Okamoto).

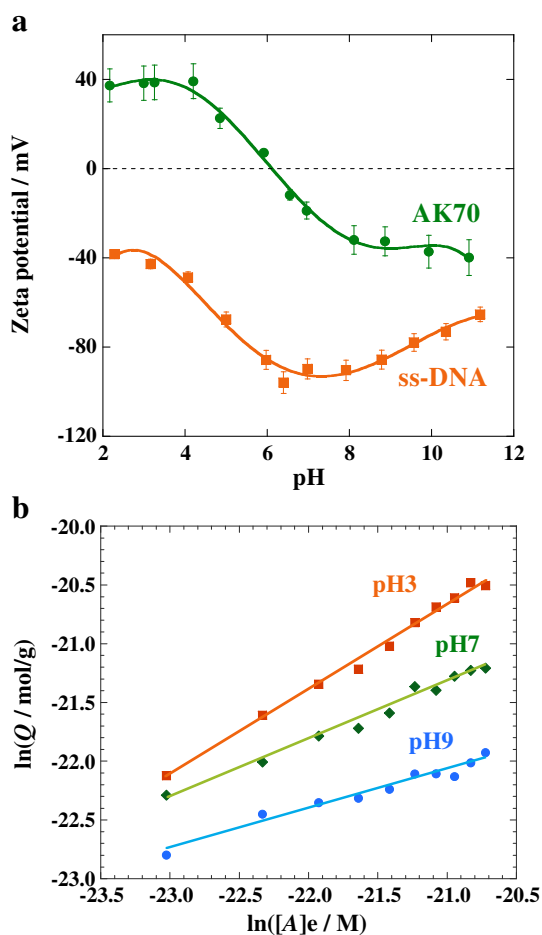


Fig. 1. (a) Zeta potential versus pH of AK70 and ss-DNA. Point of zero charge of AK70 is (pH) ~6. Results are expressed as mean \pm S.D. ($n = 4$). (b) Adsorption isotherms of ss-DNA on AK70 at 25 °C at different pHs. The solid lines are calculated by a log–log linear regression.

great interest because of gene transfer, drug release, bio-adhesion (cell capture) and origins of life studies (Ferris et al., 1996; Trevors and Pollack, 2005).

In this paper, the computer simulation to provide insight into the structure and stability of ss-DNA and adenosine 5'-monophosphate (5'-AMP) was examined during adsorption by the (OH)Al(OH₂) groups, which are exposed on the wall perforations and are the source of the pH-dependent charge characteristics of allophane (Brigatti et al., 2006; Iyoda et al., 2012). This work demonstrates the ss-DNA adsorption by the allophane particles with deep insights into the morphological feature and detailed molecular level information.

2. Experimental section

2.1. Materials

The natural allophane sample was provided by Shinagawa Chemicals Ltd. and designated as AK70. Ak70 was not further purified

Table 1
Adsorption parameters of ss-DNA on AK70.

pH	K_f /mol/g mol/l ^{-1/N}	N	r^{2a}
3.0	4.53×10^{-3}	1.38	0.99
7.0	1.59×10^{-5}	2.04	0.98
9.0	3.08×10^{-7}	2.97	0.97

^a The values are calculated by a log–log linear regression.

for use. The overall size of a single allophane particle is ~5 nm with a specific surface area of 250 m² g⁻¹, which was estimated by the *t*-method (Iyoda et al., 2012; Lippens and de Boer, 1965). The functional groups (HO)Al(OH₂) exposed on the wall perforations (defects) play a significant role as active sites in the adsorption process (Brigatti et al., 2006; Yuan and Wada, 2012). The Si/Al ratio (=0.58) of the sample was determined by dissolution in an acidic ammonium oxalate solution (Iyoda et al., 2012; Theng et al., 1982).

Based on the morphology of the allophane, AK70, Fig. S1 (Matsuura et al., 2013) shows the probable structure of the spherule wall, the wall perforations, and the intra-spherule void.

The ss-DNA taken from calf thymus was purchased from Sigma-Aldrich (D8899; $M_w = 1.64 \times 10^7$ Da, 5×10^4 base). The guanine-cytosine (G-C) content was reported to be 41.9 mol%. HCl and NaOH (Nacalai Tesque) were not further purified for use.

The details of the adsorption experiments were described in previous papers (Supplementary data regarding the adsorption experiment) (Kawachi et al., 2013; Matsuura et al., 2013).

2.2. Characterization

The surface charge characteristics of AK70 or ss-DNA molecules in water (0.1 wt.%) were determined by electrophoresis (Zetasizer Nano ZS, Malvern Instruments, UK) by the technique of laser Doppler anemometry. The method involved washing AK70 several times with water and adjusting the pH of the suspension in the range of 2–11 using dilute HCl and NaOH. All measurements were performed for four replicates and averaged to get the final value (Kawachi et al., 2013).

2.3. Model construction

Molecular mechanics force field (MM3) (Scigress, v 2.5.0, Fujitsu Ltd.) (Mizuno et al., 2013) has been used. In this study, to close up the adsorption characteristics, the ss-DNA possesses four DNA nucleotides (nts) containing individual nucleotide bases (adenine (A), thymine (T), G and C) and comprising the following sequences: 5'-AGTC-3'. By taking their van der Waals radii into account, the optimization of the molecular structure was based on the minimization of the total energy of the molecular system. The charge densities of each atom were estimated by the molecular orbital (MO) program using semiempirical parametric method (PM6) charges (Scigress, v 2.5.0, Fujitsu Ltd.) (Stewart, 2007).

The unit formula of AK70 is written as (OH)₃Al₂O₃Si_{1.2}OH, showing Al/Si ratio of 1.67, and indicating the fragments having the imogolite atomic structure over a short range (Parfitt and Henmi, 1980). The fragment links to give a porous and hollow spherule. The ~0.7 nm thick spherule wall is composed of an outer Al octahedral (gibbsitic) sheet and an inner Si sheet, in which the wall structure consists of Si tetrahedral attached to three aluminol groups (Al–OH) of the gibbsite sheet and one silanol group (HOSi(OAl)₃).

The adsorption ability of allophanes is highly depended on the interactions of phosphate and Al–OH groups through protonation and deprotonation with a varying pH. For this reason, the six constitutive repeating units (CRUs) ((OH)₃Al₂O₃SiOH) were polymerized to a modeled allophane (m-All) particle having a perforation with six (OH) Al(OH₂) groups, and the overall system was built (inset in Fig. 2b). The water molecules were described by the flexible single-point charge (SPC) model (Berendsen et al., 1987).

The most crucial and important aspect of these calculations is the method selected for sampling the relevant configurational phase space. Accordingly, the conformational search was carried out through MM/MO protocol, in which the relaxed structures were subjected to repeat all the simulations (Mizuno et al., 2013; Takeshita et al., 2013).

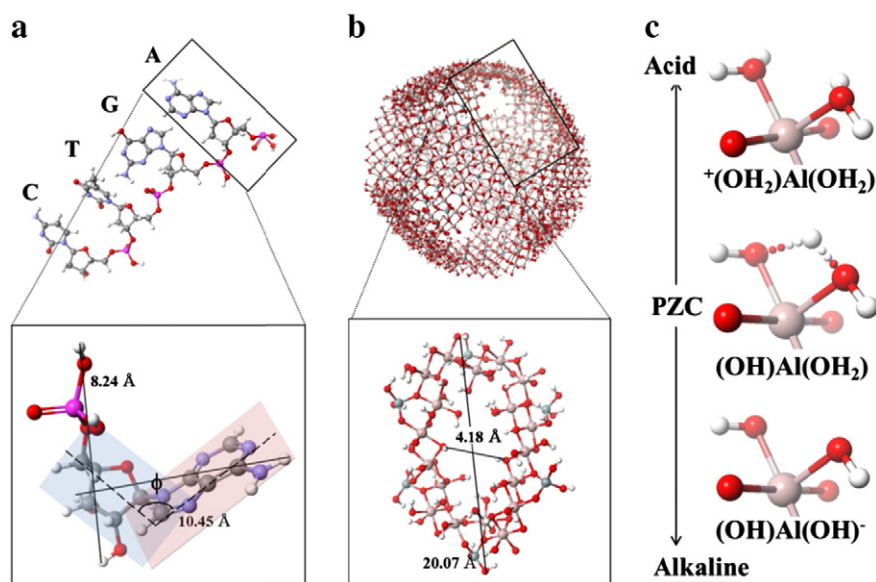


Fig. 2. (a) Configuration of ss-DNA with four DNA nts (5'-AGTC-3') and 5'-AMP before adsorption (initial state). (b) Allophane single particle with amorphous structure and modeled allophane (m-All) fragment having a perforation with six $(\text{OH})\text{Al}(\text{OH}_2)$ groups. The incompatible dimensions of the wall perforation (length of 20.07 and width of 4.18 Å) of m-All and the size of 5'-AMP (lengths of 8.24 and 10.45 Å) are constructed. (c) pH variation of active sites from acid to alkaline through PZC. For the visualization of the dihedral angle (ϕ), the deoxyribose and adenine have been shaded light blue and pink, respectively, in the inset of (a). Atom colors: O (red), H (white), C (gray), N (blue), P (pink) Si (light gray) and Al (light pink).

2.4. Adsorption enthalpy

The heat of formation using PM6, in which the dominant interactions are electrostatic, as is the case here, also calculated the adsorption enthalpy. Taking the adsorption enthalpy (ΔH_{ads}) between either ss-DNA having four DNA nts and m-All or 5'-AMP and m-All was extracted

from the final simulation snapshot. The ΔH_{ads} values are calculated by using the following equation.

$$\Delta H_{\text{ads}} = \Delta H_{\text{complex}} - (\Delta H_{\text{ss-DNA}/5'-\text{AMP}} + \Delta H_{\text{m-All}}) \quad (1)$$

where the $\Delta H_{\text{complex}}$ value is the heat of formation (in kcal/mol) of the complexes (such as ss-DNA-m-All or 5'-AMP-m-All) after adsorption, $\Delta H_{\text{ss-DNA}/5'-\text{AMP}}$ is the corresponding ss-DNA or 5'-AMP, and $\Delta H_{\text{m-All}}$, which are the isolated components, respectively.

3. Results and discussion

3.1. Surface charge characteristics

The surface charge characteristics of allophane are very different from that of ss-DNA. Allophane has a variable or pH-dependent surface charge, because the $(\text{HO})\text{Al}(\text{OH}_2)$ groups, exposed at surface defect sites, can either acquire or lose protons depending on the pH of the ambient solution. They become $^{+}(\text{OH}_2)\text{Al}(\text{OH}_2)$ by acquiring protons on the acidic side of the point of zero charge (PZC), and become $(\text{OH})\text{Al}(\text{OH})^{-}$ by losing protons on the alkaline side (Fig. 1a) (Yuan and Wada, 2012). The PZC of AK70 was (pH) ~ 6 . In the pH range of 5–7, both positively and negatively charged species are present on the surface of allophane particle. They are able to adsorb cations and anions at the same time (Yuan and Wada, 2012).

The phosphate groups of DNA molecules possess a negative charge (PO_2^{-}). The zeta potential values for the surface of the DNA are negative over the entire pH range from 2 to 11 and even more smaller negative (~ -40 mV) at a lower pH value, which may be attributed by the acquiring protons to the phosphate groups on the acidic side. Furthermore, the values decrease with increasing continuously to attain -90 mV at pH 7.0. Beyond pH 7.0, the zeta potential values increase again, presumably due to the two differently charged substituted purine groups (Schellman and Stigter, 1977).

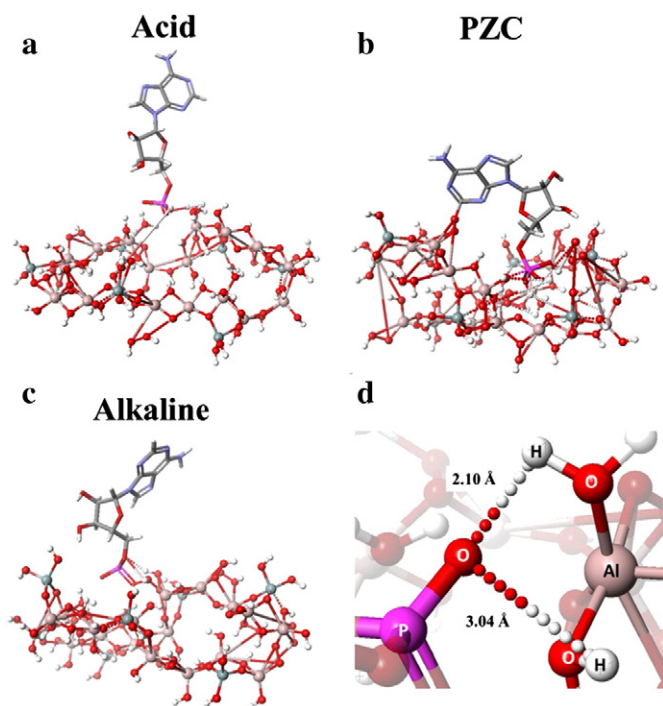


Fig. 3. Extracted configuration from the final simulation snapshot of adsorbed 5'-AMP (cylinder model) by m-All (stick and ball model) on the acid side (a), on the PZC (b), and on the alkaline side (c). (d) Two bond distances for P-O-H-O bonds (2.10 and 3.04 Å) on the acid side. Color-coding is the same as in Fig. 2.

Table 2

Heat of formation, adsorption enthalpy of complexes, and dihedral angles of adenine against the plane of 2-deoxyriboses after the complexation of 5'-AMP-m-All.

pH	Active sites	Heat of formation/kcal/mol			$\Delta H_{\text{complex}} - \Delta H_{\text{m-All}}$ kcal/mol	ΔH_{ads} kcal/mol	Dihedral angle ^a $\phi/^\circ$
		m-All	5'-AMP	Complexes			
Acidic	$^+(\text{OH}_2)\text{Al}(\text{OH}_2)$	-1394.4	-248.3	-1755.0	-360.6	-112.3	154.1
PZC	$(\text{OH})\text{Al}(\text{OH}_2)$	-3531.1		-3820.8	-289.7	-41.3	132.9
Alkaline	$(\text{OH})\text{Al}(\text{OH})^-$	-4984.1		-5096.7	-112.6	135.7	90.9

^a The angle ϕ of 5'-AMP is 113.3° in the initial state.

3.2. Adsorption capacity of ss-DNA and morphological feature

The adsorption capacity of ss-DNA decreases with increasing pH (Fig. 1b and Table 1). The adsorption isotherms were fitted by the Freundlich equation ($r^2 \geq 0.95$) (Matsuura et al., 2013). K_f is the relative adsorption capacity of the adsorbent and N is the adsorption intensity, which describes the shape of the isotherm. The adsorption isotherms exhibited a marked curvature, with slopes ($1/N$) significantly < 1.0 , indicating a convex up curvature, or L -type isotherm. The slope of the isotherms steadily decreased with increasing adsorptive concentration because the vacant sites became less accessible with the progressive covering of the adsorbent surface (Giles et al., 1960).

The functional groups exposed on the wall perforations of allophane shall be protonated with a lower pH value of the ss-DNA medium. The phosphate groups of ss-DNA possess a negative charge (PO_4^-) that bind directly to the protonated $^+(\text{OH}_2)\text{Al}(\text{OH}_2)$ groups through an electrostatic interaction leading to an increased adsorption. On the contrary, the $(\text{OH})\text{Al}(\text{OH}_2)$ groups possess a negative charge through

deprotonation with an increase in the pH of the medium. Thus the adsorption ability of allophanes is highly depended on the interactions of phosphate and $(\text{OH})\text{Al}(\text{OH}_2)$ groups through protonation and deprotonation with a varying pH.

Transmission electron microscopy (TEM) offers a qualitative understanding of the adsorption structure through direct visualization. Before adsorption on AK70, the ss-DNA exhibits a helical configuration with a width of ~ 10 nm (Matsuura et al., 2013). A single ss-DNA molecule isolated from entangled molecules is highly flexible and continuous over lengths of several micrometers. After the adsorption of ss-DNA molecules on AK70 at pH 7.0, typically discrete ss-DNA, ~ 300 nm in length, accompanied by clustered allophane particle with a width of ~ 20 nm on the surface of ss-DNA molecule was observed (Fig. S2a), which possibly represented individual ss-DNA molecule adsorbed on AK70 surface. Interconnected discrete chains associated with the condensation of the allophane clusters could also be observed (Fig. S2b). The interstitial spaces of the cluster may play an important role in the adsorption of ss-DNA molecules. The clustered allophane particles may lead to the formation of network structure as well as bundled thicker strand.

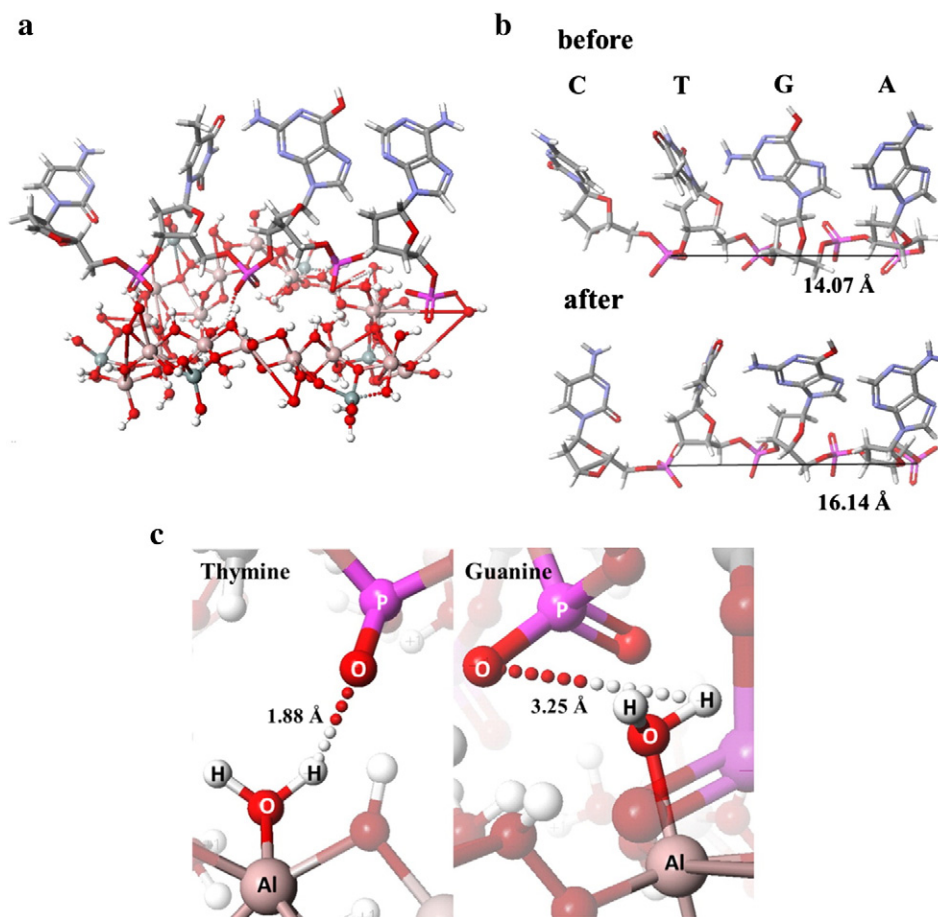


Fig. 4. (a) Extracted configuration from the final simulation snapshot of ss-DNA (5'-AGTC-3') (cylinder model) adsorbed by m-All (stick and ball model) on the acidic side. (b) Close up of the configuration of ss-DNA before (upper) and after (lower) adsorptions. m-All has been hidden to increase clarity. (c) Two P-O-H-O distances (1.88 for (T)-nt and 3.25 Å for (G)-nt). Color-coding is the same as in Fig. 2.

Table 3

Heat of formation and dihedral angles of bases against the plane of 2-deoxyriboses of ss-DNA before and after adsorptions.

Molecules	Heat of formation/kcal/mol	Bases	$\phi/^\circ$
ss-DNA (initial state)	−662.0	A: adenine	123.6
		G: guanine	144.3
		T: thymine	84.5
		C: cytosine	125.7
ss-DNA–m-All (pH acidic)	−4785.3 (−3390.9) ^a [−2729.0] ^b [−1364.5] ^c	A	132.1
		G	99.6
		T	85.7
		C	131.1
ss-DNA–m-All (PZC)	−6485.3 (−1993.2) ^a [−1178.5] ^b [−589.3] ^c	A	90.1
		G	94.8
		T	65.2
		C	104.4
ss-DNA–(H ₂ O) ₄ (pH 7)	−1289.1 (−1053.0) ^a [−389.9] ^b [−97.5] ^d	A	124.9
		G	98.9
		T	72.6
		C	114.1

^a The value (in kcal/mol) in the parenthesis is calculated from ($\Delta H_{\text{complex}} - \Delta H_{\text{m-All}}$).^b The value (in kcal/mol) in the bracket is an adsorption enthalpy (ΔH_{ads}) calculated by Eq. (1).^c The value (in kcal/mol) in the bracket is an adsorption enthalpy (ΔH_{ads}) per one bonding.^d The value (in kcal/mol) in the bracket is an adsorption enthalpy (ΔH_{ads}) per one water molecule.

For the aforementioned discussion, the numerical value of $1/N$ indicates that adsorption capacity is only slightly suppressed at lower equilibrium concentrations. This isotherm does not predict any saturation of the ss-DNA by the clustered allophane particles: thus infinite surface coverage is predicted (Hasany et al., 2002). This reasoning is consistent with the adsorption morphologies as expected. The formation of the interaction between PO_4^- groups of ss-DNA and AK70 surfaces has been revealed by Fourier transform infrared (FTIR) analysis (Matsuura et al., 2013).

3.3. Adsorption enthalpies of 5'-AMP and ss-DNA on m-All

To understand the generic adsorption in terms of the electrostatic attraction between AK70 and negatively charged phosphate (PO_4^-) groups along the backbone of the DNA single strand and/or 5'-AMP, the molecular structures of 5'-AMP and ss-DNA (Fig. 2a) were proposed. For the generation of accurate model amorphous structure allophane single particle (m-All) (Fig. 2b and inset), the CRU ($(\text{OH})_3\text{Al}_2\text{O}_3\text{SiOH}$) was built and its geometry optimized by energy minimization. Here we compare our results obtained from the simulation of the systems having positively charged ($^+(\text{OH}_2)\text{Al}(\text{OH}_2)$), negatively charged ($(\text{OH})\text{Al}(\text{OH})^-$) sites and $(\text{OH})\text{Al}(\text{OH}_2)$ as a neutral site on the PZC (Fig. 2c).

The inset in Fig. 2a shows the conformation of 5'-AMP before adsorption by m-All. Taking the corresponding configuration between 5'-AMP and the active sites of m-All the stable configuration based on the minimization of the total energy was extracted from the final simulation snapshot (Fig. 3a–c). Clearly, the active site of $(\text{OH})\text{Al}(\text{OH}_2)$ groups significantly alter the conformation of 5'-AMP with a varying pH as compared to the corresponding structure in the initial state. The conformation is conserved over the duration of MO simulation, indicating that the minimization of the total energy regarding the heat of formation is arisen from adopting this new configuration consisted of the base (adenine), 2-deoxyribose (sugar) and the phosphate group.

The calculated results show that the adsorption enthalpy (ΔH_{ads}) value of the complexation on the acidic site is strongly attractive as compared with that of the complexation on the PZC (Table 2). However, both complexations are more stable than the isolated m-All itself. Naturally those values are much greater than that of the cohesive energy (~ 5 kcal/mol) in case of the physical adsorption (Okada et al., 2005). On the other hand, the ΔH_{ads} value on the alkaline side shows a positive

value, indicating that the strong repulsive force is generated between phosphate group in 5'-AMP and $(\text{OH})\text{Al}(\text{OH})^-$ active site.

The calculation results of the energies appear somewhat qualitative, as the heat of formation does not directly relate to a heat of adsorption. In this regard, the difficulty in MO simulation of the present system and limitations of the model and methods may have been arisen. This discussion is beyond the objective of this paper, and it will be reported separately by using MO simulation equipped with the newest semiempirical method such as PM7 with dispersion function.

On the acidic side, PM6 predicts the bond distances to be 0.210 and 0.304 nm for two P–O–H–O bonds (Fig. 3d). This does not involve the formation of an inner-sphere complex through a ligand-exchange reaction between $(\text{OH})\text{Al}(\text{OH}_2)$ and phosphate groups ($(\text{HO})_2\text{OP}=\text{O}$ for 5'-AMP), which was proposed by Hashizume and Theng (2007).

For the visualization of the dihedral angle (ϕ) between 2-deoxyribose and adenine, the deoxyribose and base have been shaded light blue and light pink, respectively (inset in Fig. 2a). The estimated angle ϕ of the base against the plane of the 2-deoxyribose exhibits a certain inclination of 113.3° in the initial state (Table 2). On the acidic side (at a lower pH), the inclination of the dihedral angle shows a large value (154.1°), then the angle decreases up to 90.9° (much smaller than that of the initial state) on the alkaline side (at a higher pH). These values display the extent of the differences caused by the stabilized structure after adsorption on m-All. Those structures can be discerned from the heat of formation that may be calculated in terms of the difference between $\Delta H_{\text{complex}}$ and $\Delta H_{\text{m-All}}$ values (Eq. (1)), displayed in Table 2. The strong complexation might affect the conformation of the phosphate group and hence the base–sugar distance and the excluded volume correlation.

Another interesting feature is that the defect site on the PZC exhibits another complexation between purine and O–Al group of m-All (Fig. 3b). For the case of adenine without the phosphate group, this implies the evidence for some possibility of the interaction between adenine ring and allophane particles via the combination of electrostatic forces. The results have been demonstrated in our previous paper (Iyoda et al., 2012).

Fig. 4b (upper) shows the proposed conformation of the ss-DNA with four DNA nts (5'-AGTC-3') before adsorption. After complexation with m-All, the strand undergoes some extent of the elongation and then the configurations of the bases, 2-deoxyribose and the phosphate backbone are altered (Fig. 4a, b (lower) and angles ϕ in Table 3). As expected, the DNA strand interacts strongly with the active site on the acidic side. As seen in greater enthalpy (-3390.9 kcal/mol) calculated from ($\Delta H_{\text{complex}} - \Delta H_{\text{m-All}}$), the positively charged $^+(\text{OH}_2)\text{Al}(\text{OH}_2)$ having a large ion size might alter the structure of the DNA strand because of the more stable complexation (Table 3). These results confirm the importance of the complexation in changing the DNA structure. For this reason, the repositioning of the individual nucleotide before and after adsorptions by the active site on the acidic side (Fig. 4b) could be observed. The addition of the positively charged $^+(\text{OH}_2)\text{Al}(\text{OH}_2)$ to the ss-DNA leads to a significant increase in ΔH_{ads} (-2729.0 kcal/mol) as well as $\Delta H_{\text{complex}}$ (-4785.3 kcal/mol) (Table 3) on the acidic side. The enhanced interaction gained through complexation adds considerably to the adsorption of ss-DNA to the allophane particle. As mentioned above, with PM6 (not PM7) the trends obtained are reasonable.

PM6 predicts the distance between two phosphate groups through 5'- and 3'-terminal sequences to be 16.14 Å as compared to that of the initial state (14.07 Å, displayed in Fig. 4b (upper)). Our simulation also predicts the two bond distances for P–O–H–O to be 1.88 for (T)-nt and 3.25 Å for (G)-nt, respectively (Fig. 4c). The former distance seems to be stabilized and is much shorter than those of 5'-AMP adsorption due to the orientation of approach of ss-DNA to the active site and the ss-DNA effectively pinned to the site by the two phosphate groups. The angle ϕ for (G)-nt also is discerned from the strong adsorption by m-All. The elongation of the phosphate backbone induces the alteration

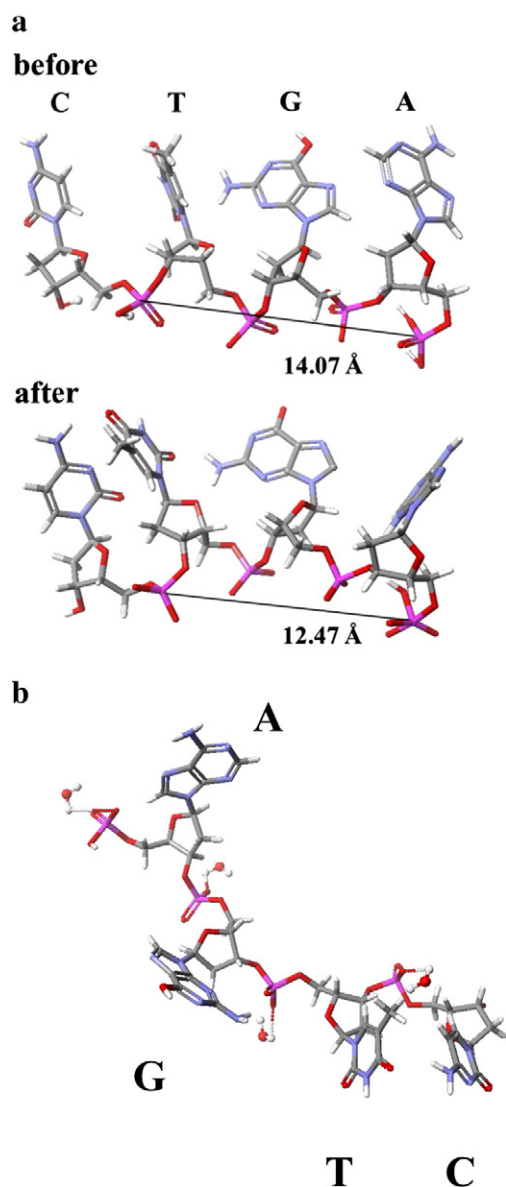


Fig. 5. (a) Extracted configuration from the final simulation snapshot of ss-DNA (5'-AGTC-3') (cylinder model) adsorbed by m-All on the PZC. Close up of the configuration of ss-DNA before (upper) and after (lower) adsorptions. m-All has been hidden to increase clarity. (b) Configuration of ss-DNA with four DNA nts (5'-AGTC-3') (cylinder model) after complexation with four H₂O molecules (stick and ball model) at pH 7 extracted from the final simulation snapshot. Color-coding is the same as in Fig. 2.

of the base–base distance and excluded volume correlation among bases.

The strong adsorption enthalpy is a main factor in determining the effectiveness of the interface in the complexation, accompanied by the large exothermic per one bonding (−1364.5 kcal/mol). This value is one order of magnitude greater than that of 5'-AMP adsorption by m-All (−112.3 kcal/mol, displayed in Table 2). Owing to the significant difference between ss-DNA molecular and the allophane cluster size (Fig. 2a, b), and the incompatible dimensions of the wall perforation and one nt, most of the nts on the phosphate backbone could not act as the active sites.

As described earlier, on the acidic side (pH < PZC), we postulate that the negatively charged PO₂[−] groups along the backbone of the ss-DNA interact with the positively charged (⁺(OH₂)Al(OH₂)) sites of AK70 and subsequently the larger adsorption capacity of ss-DNA is led

associated with lower energy barrier as well when compared with those on the PZC (Fig. 5a and Table 3). On the PZC, the same features are seen in the corresponding case of 5'-AMP–m-All complexation after adsorption. That is, the ΔH_{ads} value of the complexation on the PZC becomes half as compared with that of the MO simulation on the acidic site. The main difference is the phosphate backbone adopts a more compact conformation as compared with the extended structure of the 5'-AGTC-3' on the acidic side. The distance between two phosphate groups through 5'- and 3'-terminal sequences is 12.47 Å presumably due to the weak adsorption enthalpy. The visualizations in Fig. 4b show the lying more flat on the positively charged (⁺(OH₂)Al(OH₂)) sites.

The result obtained from the complexation with water molecules was compared. The calculated result shows that the ΔH_{ads} (−97.5 kcal/mol per one water molecule) in ss-DNA–(H₂O)₄ is less attractive as compared with that of ss-DNA–m-All (Fig. 5b and Table 3). The ΔH_{ads} value on the alkaline side could not be obtained due to the convergence problem.

4. Conclusions

In the present study, the adsorption capacity of ss-DNA (K_f) which decreases with increasing pH due to the interaction generated between phosphate groups of ss-DNA and functional (OH)Al(OH₂) groups through deprotonation has been demonstrated. The molecular orbital (MO) computer simulation has been used to probe the interaction of ss-DNA and/or 5'-AMP and AK70 with active sites. For the complexation of 5'-AGTC-3' on m-All, our simulations predicted that the strand undergoes some extent of the elongation, which induces the alteration of the conformation of the phosphate backbone, base–base distance and excluded volume correlation among bases. The interpretation of experimental studies was supported through detailed molecular level information.

Author contributions

M.O. planned the study. Y.M. and S.A. performed adsorption and characterization experiments. Y.M. carried out the computer simulation and analyzed the data with the help of S.A. and M.O. The manuscript was written through contributions of all authors. All authors have given approval to the final version of the manuscript.

Conflict of interest

The authors declare no competing financial interest.

Acknowledgments

This work was supported by the Grant in TTI as a Special Research Project (2013–14) and the Strategic Research Infrastructure Project of the Ministry of Education, Sports, Science and Technology, Japan (S1001037) (2010–14).

Appendix A. Supplementary data

Supplementary data to this article can be found online at <http://dx.doi.org/10.1016/j.clay.2014.09.023>.

References

- Berendsen, H.J.C., Grigera, J.R., Straatsma, T.P., 1987. The missing term in effective pair potentials. *J. Phys. Chem.* 91, 6269–6271.
- Brigatti, M.F., Galan, E., Theng, B.K.G., 2006. Structures and mineralogy of clay minerals. In: Bergaya, F., Theng, B.K.G., Lagaly, G. (Eds.), *Handbook of Clay Science*. Elsevier, Amsterdam, pp. 19–86.
- Cleaves II, H.J., Crapster-Pregont, E., Jonsson, C.M., Jonsson, C.L., Sverjensky, D.A., Hazen, R.A., 2011. The adsorption of short single-stranded DNA oligomers to mineral surfaces. *Chemosphere* 83, 1560–1567.

- Dworkin, J.P., Lazcano, A., Miller, S.L., 2003. The roads to and from the RNA world. *J. Theor. Biol.* 222, 127–134.
- Ferris, J.P., Hill, A.R., Liu, R.H., Orgel, L.E., 1996. Synthesis of long prebiotic oligomers on mineral surfaces. *Nature* 381, 59–61.
- Gilbert, W., 1986. The RNA world. *Nature* 319, 618.
- Giles, C.H., MacEwan, T.H., Nakhwa, S.N., Smith, D., 1960. Studies in adsorption. Part XI. A system of classification of solution adsorption isotherms, and its use in diagnosis of adsorption mechanisms and in measurement of specific surface areas of solids. *J. Chem. Soc.* 148, 3973–3993.
- Hasany, S.M., Saeed, M.M., Ahmed, M., 2002. Sorption and thermodynamic behavior of zinc(II)-thiocyanate complexes onto polyurethane foam from acidic solutions. *J. Radioanal. Nucl. Chem.* 252, 477–484.
- Hashizume, H., Theng, B.K.G., 2007. Adenine, adenosine, ribose and 5'-AMP adsorption to allophane. *Clay Clay Miner.* 55, 599–605.
- Iyoda, F., Hayashi, S., Arakawa, S., Okamoto, M., 2012. Synthesis and adsorption characteristics of hollow spherical allophane nano-particles. *Appl. Clay Sci.* 56, 77–83.
- Joyce, G.F., 2002. The antiquity of RNA-based evolution. *Nature* 418, 214–221.
- Kawachi, T., Matsuura, Y., Iyoda, F., Arakawa, S., Okamoto, M., 2013. Preparation and characterization of DNA/allophane composite hydrogels. *Colloids Surf. B* 112, 429–434.
- Kevadiya, B.D., Joshi, G.V., Bajaj, H.C., 2010. Layered bionanocomposites as carrier for procainamide. *Int. J. Pharm.* 388, 280–286.
- Kevadiya, B.D., Patel, T.A., Jhala, D.D., Thumbar, R.P., Brambhatt, H., Pandya, M.P., Rajkumar, S., Jena, P.K., Joshi, G.V., Gadhia, P.K., Tripathi, C.B., Bajaj, H.C., 2012. Layered inorganic nanocomposites: a promising carrier for 5-fluorouracil (5-FU). *Eur. J. Pharm. Biopharm.* 81, 91–101.
- Lippens, B.C., de Boer, J.H., 1965. Studies on pore systems in catalysts: V. *J. Catal.* 4, 319–323.
- Matsuura, Y., Iyoda, F., Arakawa, S., John, B., Okamoto, M., Hayashi, H., 2013. DNA adsorption characteristics of hollow spherule allophane nano-particles. *Mater. Sci. Eng. C* 33, 5079–5083.
- Mizuno, C., John, B., Okamoto, M., 2013. Percolated network structure formation and rheological properties in nylon 6/clay nanocomposites. *Macromol. Mater. Eng.* 298, 400–411.
- Okada, K., Nishimuta, K., Kameshima, Y., Nakajima, A., 2005. Effect on uptake of heavy metal ions by phosphate grafting of allophane. *J. Colloid Interface Sci.* 286, 447–454.
- Parfitt, R.L., Henmi, T., 1980. Structure of some allophanes from New Zealand. *Clay Clay Miner.* 28, 285–294.
- Saeki, K., Sakai, M., Wada, S.I., 2010. DNA adsorption on synthetic and natural allophanes. *Appl. Clay Sci.* 50, 493–497.
- Schellman, J.A., Stigter, D., 1977. Electrical double layer, zeta potential and electrophoretic charge of double-stranded DNA. *Biopolymers* 16, 1415–1434.
- Silva, G.R., Ayres, E., Orefice, R.L., Moura, S.A., Cara, D.C., Cunha Ada Jr., S., 2009. Controlled release of dexamethasone acetate from biodegradable and biocompatible polyurethane and polyurethane nanocomposite. *J. Drug Target.* 17, 374–383.
- Stewart, J.J.P., 2007. Optimization of parameters for semiempirical methods V: modification of NDDO approximations and application to 70 elements. *J. Mol. Model.* 13, 1173–1213.
- Stotzky, G., 2000. Persistence and biological activity in soil of insecticidal proteins from *Bacillus thuringiensis* and of bacterial DNA bound on clays and humic acids. *J. Environ. Qual.* 29, 691–705.
- Takeshita, T., Matsuura, Y., Arakawa, S., Okamoto, M., 2013. Biomineralization of hydroxyapatite on DNA molecules in SBF: morphological features and computer simulation. *Langmuir* 29, 11975–11981.
- Taylor, D.H., Wilson, A.T., 1979. The adsorption of yeast RNA by allophane. *Clay Clay Miner.* 27, 261–268.
- Theng, B.K.G., Russell, M., Churchman, G.J., Parfitt, R.L., 1982. Surface properties of allophane, halloysite, imogolite. *Clay Clay Miner.* 30, 143–149.
- Trevors, J.T., Pollack, G.H., 2005. Hypothesis: the origin of life in a hydrogel environment. *Prog. Biophys. Mol. Biol.* 89, 1–8.
- Wächtershäuser, G., 2006. From volcanic origins of chemoautotrophic life to Bacteria, Archaea and Eukarya. *Philos. Trans. R. Soc. Lond. B* 361, 1787–1808.
- Wilson, M.J., 1999. The origin and formation of clay minerals in soils: past, present and future perspectives. *Clay Miner.* 34, 7–25.
- Yuan, G., Wada, S.I., 2012. Allophane and imogolite nanoparticles in soil and their environmental applications. In: Barnard, A.S., Guo, H.B. (Eds.), *Nature's Nanostructures*. Pan Stanford Publishing Pte. Ltd., Singapore, pp. 485–508.
- Yuan, Q., Shah, J., Hein, S., Misra, R.D.K., 2010. Controlled and extended drug release behavior of chitosan-based nanoparticle carrier. *Acta Biomater.* 6, 1140–1148.